Arabian Journal of Chemistry (2022) **15**, 103600

King Saud University

Arabian Journal of Chemistry

www.ksu.edu.sa
www.sciencedirect.com

ORIGINAL ARTICLE

Computational screening and biochemical analysis of *Pistacia integerrima* and *Pandanus odorifer* plants to find effective inhibitors against Receptor-Binding domain (RBD) of the spike protein of SARS-Cov-2

Gobindo Kumar Paul [a,1], Shafi Mahmud [a,1], Afaf A Aldahish [b], Mirola Afroze [c], Suvro Biswas [a], Swagota Briti Ray Gupta [a], Mahmudul Hasan Razu [c], Shahriar Zaman [a], Md. Salah Uddin [a], Mohammed H Nahari [d], Mohammed Merae Alshahrani [d], Mohammed Abdul Rahman Alshahrani [d], Mala Khan [c,*], Md. Abu Saleh [a,*]

[a] *Microbiology Laboratory, Department of Genetic Engineering and Biotechnology, University of Rajshahi, Rajshahi 6205, Bangladesh*
[b] *Department of Pharmacology and Toxicology, College of Pharmacy, King Khalid University, Abha 62529, Asir, Saudi Arabia*
[c] *Bangladesh Reference Institute for Chemical Measurements, BRiCM, Bangladesh Council of Scientific and Industrial Research, Dhanmondi, Dhaka 1205, Bangladesh*
[d] *Department of Clinical Laboratory Sciences, Faculty of Applied Medical Sciences, Najran University, PO Box 1988, Najran 61441, Saudi Arabia*

Received 29 August 2021; accepted 25 November 2021
Available online 1 December 2021

KEYWORDS

Plant extracts;
SARS-CoV-2;
Antioxidant;

Abstract Although World Health Organization-approved emergency vaccines are available in many countries, the mortality rate from COVID-19 remains high due to the fourth or fifth wave and the delta variant of the coronavirus. Thus, an effective mechanistic investigation in treating this disease is urgently needed. In this work, we extracted phytochemicals from two mangrove plants,

* Corresponding authors.
E-mail addresses: malakhan_07@yahoo.com (M. Khan), saleh@ru.ac.bd (Md. Abu Saleh).
[1] Co-First Author.

Peer review under responsibility of King Saud University.

Production and hosting by Elsevier

https://doi.org/10.1016/j.arabjc.2021.103600

Cytotoxicity;
Receptor-binding Domain;
Molecular Dynamics Simulation

Pistacia integerrima and *Pandanus odorifer*, assessing their potential actions against the receptor-binding domain (RBD) of the spike protein of SARS-CoV-2. The antioxidant activities of *Pistacia integerrima* leaves and fruits were 142.10 and 97.13 μg/mL, respectively, whereas *Pandanus odorifer* leaves and fruits were 112.50 and 292.71 μg/mL, respectively. Furthermore, leaf extracts from both plants had lower cytotoxicity against *Artemia salina* than fruit extracts. Gas chromatography-mass spectrometry analysis revealed a total of 145 potential phytochemicals from these extracts. Three phytochemicals, 28-demethyl-beta-amyrone, 24-Noroleana-3,12-diene, and stigmasterol, displayed binding free energy values of − 8.3, −7.5, and − 8.1 Kcal/mol, respectively, in complexes with the spike protein of SARS-CoV-2. The root-mean-square deviation, solvent-accessible surface area, radius of gyration, root-mean-square fluctuations, and hydrogen bonds were used to ensure the binding stability of the docked complexes in the atomistic simulation. Thus, wet-lab validations are necessary to support these findings.

1. Introduction

The SARS-CoV-2 virus, which causes the disease known as COVID-19, is highly contagious. Initially identified in Wuhan Province, China, on December 20, 2019, the World Health Organization (WHO) labeled the outbreak a pandemic after a significant global epidemic (C. et al., 2020; Ebrahim et al., 2020). The virus shares the highest (87.6–89%) nucleotide sequence similarity with bat-SL-CoVZC45. SARS-CoV and MERS-CoV share 79.0% identity and 51.8% uniformity (Machhi et al., 2020). The spike (S), envelope (E), membrane (M), and nucleocapsid (N) proteins are all encoded by the SARS-CoV-2 genome (Mahmud et al., 2021c; Satarker and Nampoothiri, 2020). Due to their important function in viral binding, fusion, and entry into the host cell via interaction with the ACE-2 (Angiotensin-Converting Enzyme-2) receptor, the S (spike) glycoprotein of SARS-CoV-2 has been proposed as an appealing target for generating novel vaccines and drugs (He et al., 2004).

It was discovered that SARS-CoV-2 uses its unusual S protein to link with angiotensin-converting enzyme 2 as a functional receptor for viral entry (Kim et al., 2021; Li et al., 2005; Shang et al., 2020). The S protein appears as a homotrimer on the virus structure. The RBD-containing S1 subunit is responsible for viral coalition and entry into the host cell, whereas the S2 subunit moderates cell membrane unification upon proteolytic activation (Kim et al., 2021; Shang et al., 2020; Yuan et al., 2021). Two proteolytic cleavage sites are impending at the S1/S2 border and in S2 immediately prior to the fusion peptide. The S1 domain comprises a receptor-binding domain and an N-terminal domain (NTD) that interact with two SD1 and SD2 subdomains at the C-terminus. As the receptor-binding site (RBS) is partially sequestered in the down state, the RBD fluctuates between an up and a down state and can only be linked to ACE2 in an upstate (Yuan et al., 2021).

The core section of the SARS-CoV-2 receptor-binding domain is composed of a twisted antiparallel sheet with five strands named β1, β2, β3, β4, and β7, with sparse copulative loops and helices. Between the strands of β4 and β7, there is an elongated embodiment that bears the concise β6 and β5 strands as well as α5 and α4 loops and helices. The receptor-binding motif (RBM) is an extended manifestation of the virus's maximal contracting residues that attach to ACE2. Nine cysteine residues are found in the RBD, eight of which form four pairs of disulfide bonds: three (Cys391–Cys525, Cys336–Cys361, Cys379–Cys432) are in the core segment of the RBD, which aid in β sheet formation stagnation and the remaining pair (Cys480–Cys488) appends the loops in the RBM's far edge. The peptide substrate-binding site is formed by the interaction of two lobes in the N-terminal peptidase domain of the ACE2 receptor. The quadrant flank of the pony lobe of ACE2 in the SARS-CoV-2 RBD coalesces in the expanded RBM, which integrates the N-terminal helix of ACE2 with a concave outward periphery in the RBM (Lan et al., 2020). This process suggests that the RBD of the S protein could be a promising target for blocking virus fusion or binding to the ACE2 receptor in the host cell, which could be a key target for the development of therapeutics and vaccines (Corrêa Giron et al., 2020).

Medicinal plants contain an extensive diversity of secondary metabolites that have a wide range of biological activities (A. Hussein and A. El-Anssary, 2019). In this study, we chose two mangrove plants with antimicrobial activities, *Pistacia integerrima* and *Pandanus odorifer* (Pant and Samant, 2010) for virtual screening to identify a potential compound that can inhibit the target protein of SARS-CoV-2. Molecular docking and molecular dynamics simulations were performed to confirm the binding posture and orientations discovered in the docking study.

2. Experimental

2.1. Sample collection

The leaves and fruits of *Pistacia integerrima* and *Pandanus odorifer* plants were collected from a mangrove forest in Dacope Upazila, Khulna, Bangladesh, and disease-free samples were placed in a sterile zip bag for transport to the Microbiology Laboratory, Department of Genetic Engineering and Biotechnology, University of Rajshahi, Rajshahi, Bangladesh, for further analysis.

2.2. Preparation of extracts

Separately, the obtained samples were rinsed with running tap water to remove adhering particles before being dried in an incubator at 60 °C. Afterward, an electric grinder machine

was used to grind each sample individually (Jaipan, Family mate, Mumbai, India). Methanolic extracts were made using the procedure reported by Liu et al. (2008), in which 25 g of ground extracts were soaked in 100 mL methanol solvent and shaken continuously for 7 d at 25 °C in a shaker. The extracts were then filtered using Whatman No. 1 filter paper and allowed to evaporate at room temperature (Wavare et al., 2017). After evaporation, the yield of each extract was 1.95 g, 1.87 g, for *Pistacia integerrima* leaves and fruits and 1.07 g, 1.17 g for *Pandanus odorifer* leaves and fruits. The extracts were then kept at 4 °C in an airtight container until needed.

2.3. Antioxidant activity test

The antioxidant activity was estimated using DPPH (2,2-Dip henyl-1-Picryl-Hydrazyl-Hydrate) free radical scavenging assay established by Ilahi et al. (2013) with BHT (Butylated Hydroxy Toluene) as a standard (Sharma and Bhat, 2009). The BHT concentration was adjusted to 50, 100, 150, 200, and 250 µg/mL. The entire amount was then increased to 1 mL by adding methanol, followed by 2.5 mL of DPPH solution. After 30 min of conditioning at room temperature, the optical density was measured at 517 nm using a UV–visible spectrophotometer (Analytik Jena, Germany). The percentage of DPPH scavenging capacity was estimated using the formula Mahmud et al. (2021a), and the IC50 value was computed using a linear scatter graph in Microsoft Excel 2010.

2.4. Cytotoxicity test

An in vitro cytotoxicity test was conducted according to the method described by Achakzai et al. (2019) using *Artemia salina* (brine shrimp nauplii). Briefly, *Artemia salina* were hatched at room temperature in a particular tank, and the extract concentration of 25, 50, 100, 150, 200, and 250 µg/mL were placed in tubes. Next, 15 larvae were put in each test tube with 10 mL of artificially prepared seawater. Live and dead shrimps were counted after 24 h, and a lethal concentration (LC_{50}) was obtained by plotting the results on an Excel regression scatter graph.

2.5. Gas chromatography-mass spectroscopy analysis

The bioactive compounds from *Pistacia integerrima* and *Pandanus odorifer* plants leaves and fruits were analyzed using GC–MS (Shimadzu, Japan; Model GC–MS TQ 8040) analysis with an electronic ionization detector. A fused silica capillary column at a temperature of 50 °C was used (Rxi-5Sil MS, 30 m, 0.25 mm ID, and 0.25 µm). The samples were then taken in a fix split mode at 250 °C. The oven was preheated at 500 °C for 1 min, then 200 °C for 2 min, and finally 300 °C for 7 min. The ionization voltage was adjusted to 70 eV and the electron multiplier was set to 900 V. The unknown spectra of GC–MS were then compared to the spectra of existing chemicals housed in the Wiley or NIST libraries (Profiles et al., 2021). The names of the compounds, molecular formulas, and weights were then determined (A. et al., 2017).

2.6. Ligand preparation

The chemical compounds were obtained from *Pistacia integerrima* and *Pandanus odorifer* plant extracts using GC–MS analysis, and their SDF format of 3D structures were retrieved from the PubChem database (http://www.pubchem.ncbi.nlm.nih.gov/);(Kim et al., 2016). The mmff94 force field from Avogadro software was used to construct and improve the structures of the ligands (Hanwell et al., 2012).

2.7. Protein preparation

The spike receptor-binding domain of the SARS-CoV-2 structure was retrieved from Protein Data Bank (https://www.rcsb.org/) (PDB ID: 6M0J) and cleaned using Discovery Studio (Gao and Huang, 2011). Moreover, the A chain—including angiotensin converting enzyme-2 (ACE2)—was eliminated in Discovery Studio software. Next, a clean protein structure (Spike Protein S1) was minimized using the YASARA Dynamics software employing the AMBER14 force field (Land and Humble, 2018).

2.8. Molecular docking

Molecular docking of all identified compounds in *Pistacia integerrima* and *Pandanus odorifer* leaves and fruits extracts was performed using the AutoDock Vina software tool. The ligands were then converted to PDBQT format, with the box size and grid box center set to (X:26.29 Å, Y:12.60 Å, and Z:58.94 Å) and (X:50.33 Å, Y:67.27 Å, and Z:59.25 Å), respectively (Jaghoori et al., 2016; Nguyen et al., 2020; Trott and Olson, 2010). The level of thoroughness was set to 8. The total number of steps, updates steps, and energy difference for the ligand molecules were adjusted to 200, 1, and 0.1, respectively, utilizing the universal force field with conjugate gradient algorithms. The docking calculations were done with the PyRx program (version 0.8), while the binding interactions analysis was done with the Discovery Studio (version 3.0) (Gao and Huang, 2011) and PyMOL software (version 2.3) (DeLano, 2002). Furthermore, the DockThor (Santos et al., 2020) and SwissDock program (Grosdidier et al., 2011) were also used to explore the binding energy of the ligand and protein complexes. For the docking investigation, the lowest binding scores were used, and energy was estimated in Kcal/mol.

2.9. Molecular dynamics simulation

A molecular dynamics simulation study was conducted in the YASARA dynamics package in the AMBER14 force field (Land and Humble, 2018; Wang et al., 2004). The docked complexes were initially cleaned and optimized. A hydrogen bond networking system was then applied to the docked complexes. A cubic simulation cell was generated using the TIP3P solvation model in periodic boundary conditions (Harrach and Drossel, 2014). The simulation conditions were set to pH 7.4, 310 K temperature, and 0.9% NaCl. The energy minimization

of the simulation system was achieved using the steepest gradient algorithms (5000 cycles) and annealing method. The simulation system's time step was set to 2.0 fs. The long-range electrostatic interactions were calculated through the particle mesh Ewald (PME) by a cutoff radius of 8.0 Å (Essmann et al., 1995). The simulation trajectories were saved at every 100 ps interval. The final simulation was ran for 100 ns (Krieger and Vriend, 2015) while adhering to constant pressure and Berendsen thermostat. The root mean square deviation, solvent accessible surface area, radius of gyration, and hydrogen bond were studied using simulation trajectories (Afrose et al., 2021; Chowdhury et al., 2021; Mahmud et al., 2021d,e,a,f,g; Pramanik et al., 2021; Rakib et al., 2021; Uddin et al., 2021).

2.10. ADMET analysis

The Swiss ADME (http://www.swissadme.ch/) (Daina et al., 2017) and pkCSM (http://biosig.unimelb.edu.au/pkcsm/) (Pires et al., 2015) tools were used for the evaluation of the pharmacological properties of ligands where canonical SMILES of the compound were used as the entry system for absorption, distribution, metabolism, and toxicity (ADMET) calculations.

2.11. Statistical analysis

Data were analyzed by GraphPad Prism (version 8.4), and all the values are reported as the mean ± standard error of the mean (SEM). Values were regarded as significantly different at ***p less than 0.001, **p less than 0.01, and *p less than 0.05, with one-way analysis of variance (ANOVA), followed by Dunnett's test, while two-way ANOVA with repeated measures was used. The in vitro study was performed using triplicate measurements.

3. Results

3.1. DPPH scavenging activity

The free radical scavenging activities of the leaves and fruits extracts of *Pistacia integerrima* and *Pandanus odorifer* were demonstrated in **Figures 1 and S1**. The scavenging percentage of both plants' leaves and fruits extracts increased gradually as the concentration of the extracts increased. The IC_{50} value of *Pistacia integerrima* leaves and fruits were 142.10 and 173.58 µg/mL, respectively, while *Pandanus odorifer* leaves and fruits were 112.50 and 292.71 µg/mL, respectively, while the BHT standard was 145.96 µg/mL. Thus, these results specified that IC_{50} value for fruits is higher (90.37 µg/ml) than for BHT. Thus, these data signify that *Pandanus odorifer* plant leaves have the superior antioxidant activity than other extracts **(**Fig. 1**),** because it has 50% scavenging at 112.50 µg/mL, which is lower than other concentrations.

3.2. Cytotoxic activity

The cytotoxicity of these methanolic plant extracts are shown in Fig. 2 **and Figure S2**. The LC_{50} value of *Pistacia integerrima* plant leaves and fruits was 95.54 and 82.27 µg/mL, respectively, while *Pandanus odorifer* plant leaves and fruits was 117.00 and 67.51 µg/mL. Therefore, these findings clearly demonstrated that *Pandanus odorifer* plant leaves have less toxic activity than other investigated extracts **(**Fig. 2**)** since it revealed 50% mortality at 117.00 µg/mL, which was higher than other concentrations.

3.3. GC–MS analysis

Both *Pistacia integerrima* and *Pandanus odorifer* leaves had 40 compounds in GC–MS analysis, whereas fruits had 20 and 45

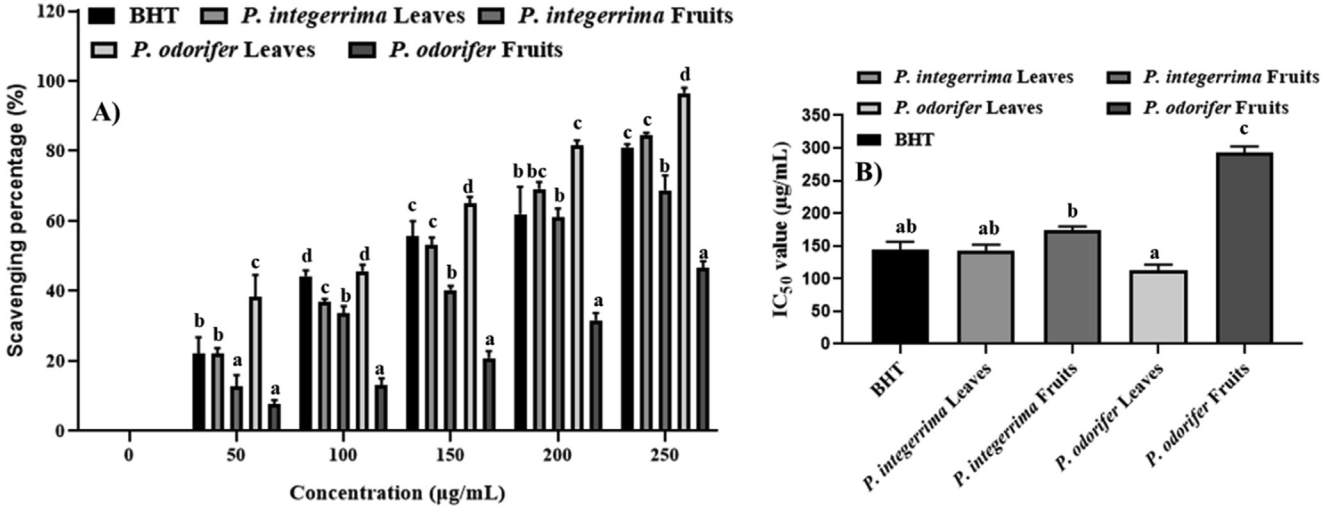

Fig. 1 Antioxidant activity of *Pistacia integerrima* and *Pandanus odorifer* plant leaves and fruits extracts. A indicates DPPH scavenging activity of all extracts from both plants and B indicates IC_{50} value of all extracts from both plants. Different significant letters indicate significant differences between mean ± SD of replications (n = 3) at a $P \leq 0.05$ significant level.

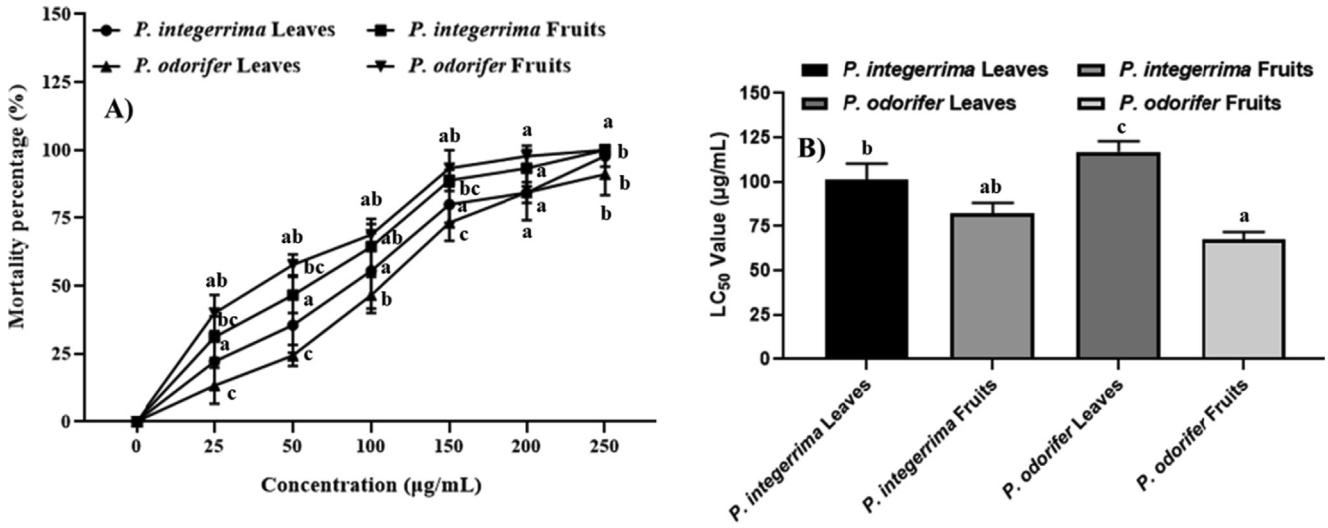

Fig. 2 Cytotoxic activity of *Pistacia integerrima* and *Pandanus odorifer* plant leaves and fruits extract against brine shrimp. A indicates the mortality percentage of both plant's leaves and fruits extracts and B indicates LC_{50} value of all extracts from both plants. Variations in significant letters indicate significant differences between mean ± SD of replications (n = 3) at a $p \leq 0.05$ significance level.

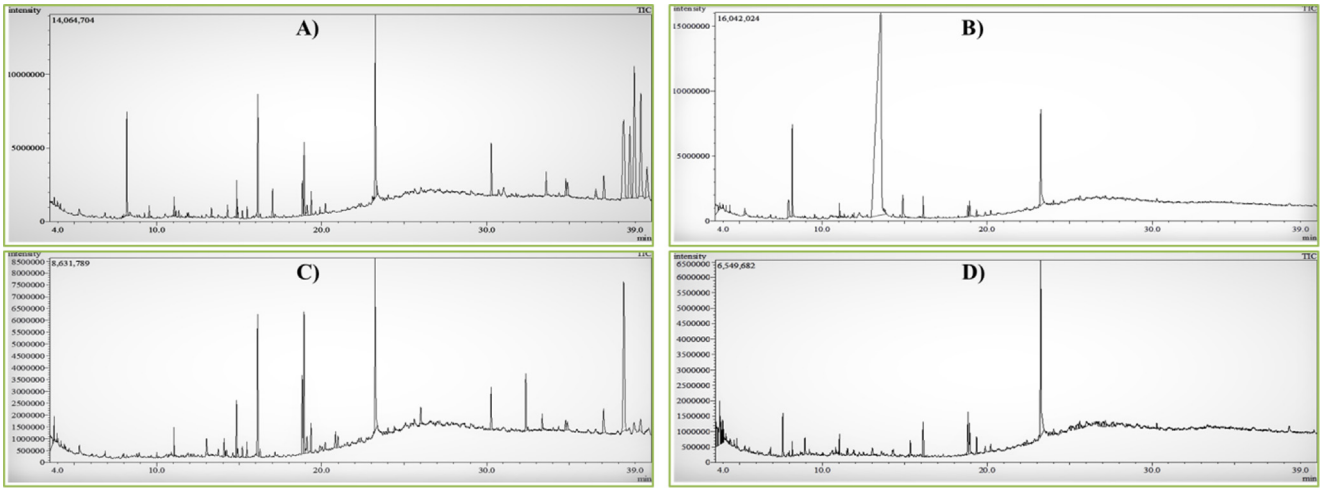

Fig. 3 GC–MS chromatogram of *Pistacia integerrima* and *Pandanus odorifer* plant extract. A and B indicate GC–MS chromatogram of *Pistacia integerrima* plant leaves and fruits extracts respectively and C and D indicate chromatogram of *Pandanus odorifer* plant leaves and fruits extracts, respectively.

compounds, respectively (Fig. 3 and S3-S6). The International Union of Pure and Applied Chemistry name, molecular formula, canonical SMILES, and retention time of the compounds are presented in Table S3-S6. The major compounds of *Pistacia integerrima* leaf extracts are Lup-20(29)-en-3-ol, acetate, (3.beta.) ($C_{32}H_{52}O_2$) has the highest concentration (15.24%), followed by beta-sitosterol ($C_{29}H_{50}O$) with 13.29%, 24-Noroleana-3,12-diene ($C_{29}H_{46}$) with 12.32%, 9-octadecenamide, (Z) ($C_{18}H_{35}NO$) with 10.75%. The most prominent compounds of *Pistacia integerrima* fruit extracts include 4-O-Methylmannose ($C7H_{14}O_6$) with the highest proportion (79.26%), followed by 9-octadecenamide, (Z) ($C_{18}H_{35}NO$) with 6.78% and 8-Azabicyclo [3.2.1] octan-3-ol, 8-methyl-, endo ($C_8H_{15}NO$) with 3.72%. Furthermore, the most abundant chemicals in *Pandanus odorifer* leaf extracts are 28-demethyl-beta-amyrone ($C_{29}H_{46}O$), which accounts for 39.24%, gamma-sitosterol ($C_{29}H_{50}O$) with 38.17%, and stigmasterol ($C_{29}H_{48}O$) with 37.00%. Moreover, the most significant components of *Pandanus odorifer* leaf extracts are *trans*-geranylgeraniol ($C_{20}H_{34}O$) with 30.27%, 3–cyclohexenecarboxylic acid, 6,6-dimethyl-4-(4-morpholyl)-2-oxo-meth yl ester ($C_{14}H_{21}NO_4$) with 27.64%, and 5-methyl-Z-5-docosene ($C_{23}H_{46}$) with 27.15%.

3.4. Docking analysis

Molecular docking analysis was carried out to explore the binding interaction and identify lead molecules with a higher affinity for SARS-Cov-2 spike receptor-binding domain. The three compounds (Fig. 4); 28-demethyl-beta-amyrone, 24-Noroleana-3,12-diene, and stigmasterol had a binding energy

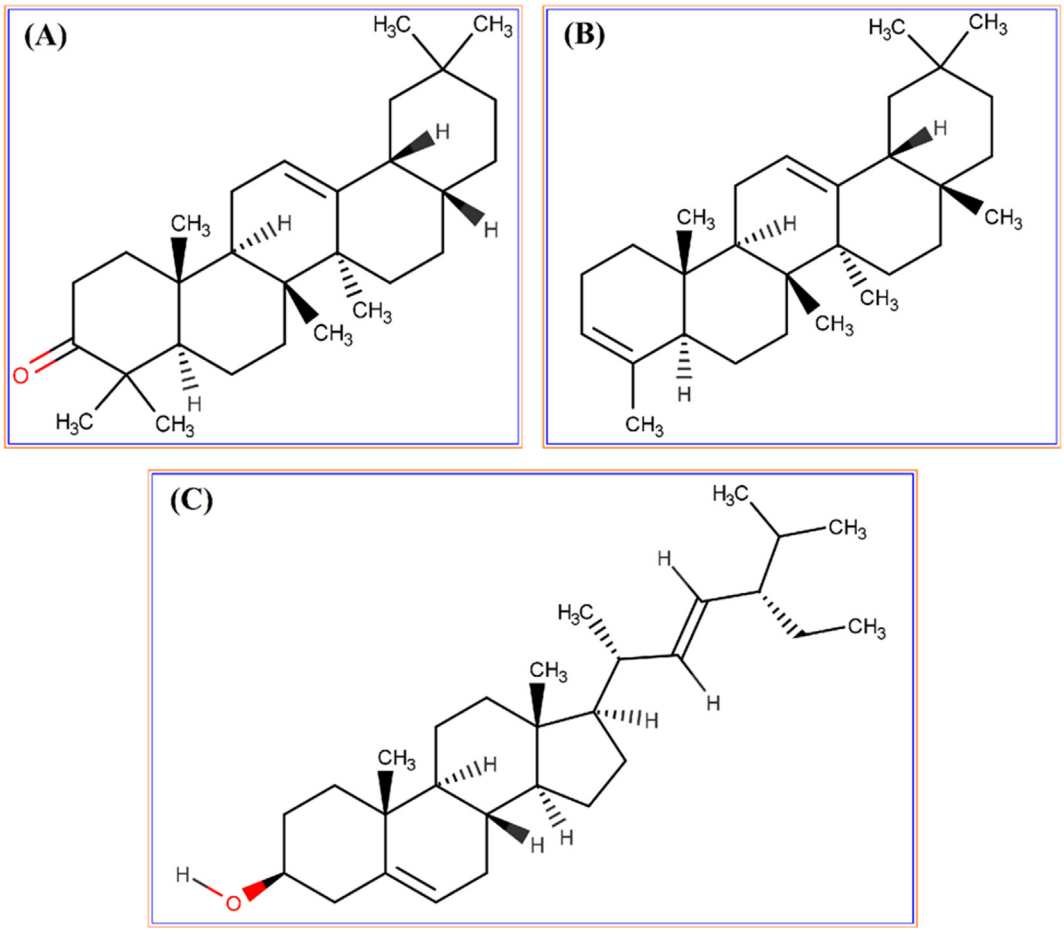

Fig. 4 Two-dimensional (2D) chemical structures of (A) 28-demethyl-beta-amyrone, (B) 24-Noroleana-3,12-diene, and (C) stigmasterol. The structures were drawn by using the Marvin Sketch software.

of − 8.3, −7.5, −8.1 Kcal/mol, respectively **(**Table 1**),** which is higher than the other compounds of *Pistacia integerrima* and *Pandanus odorifer* plants. Moreover, the DockThor and SwissDock program was also employed to further validate the docking energy where 28-demethyl-beta-amyrone, 24-Noroleana-3,12-diene, and stigmasterol had − 5.985, −6.002, −5.712 Kcal/mol energy in DockThor and − 7.38, −7.48, −7.25Kcal/-mol, respectively, in SwissDock. Regarding the compounds, 28-demethyl-beta-amyrone had two Pi-alkyl interactions at Phe374, Phe342, and an alkyl bond at Leu368, as well as a Pi-sulfur bond at Trp436 residues (Fig. 5**)**. The 24-Noroleana-3,12-diene and spike protein domain-receptor complexes were stabilized by two alkyl bonds at Val367, Leu368, three pi-alkyl bonds at Phe374, Phe342, and one Pi-sulfur bond at Phe342 (Fig. 6**)**. Moreover, the stigmasterol had two pi-alkyl interactions points at Leu335 and Leu368 residues, whereas three pi-alkyl bonds at Phe374, Phe342, and Phe338 residues (Fig. 7**)**.

3.5. ADMET analysis

The ADMET calculations were used to adjudicate the drug-likeness properties of the selected three compounds **(**Table 2 **and Tables S7.1–S7.4)**. According to the Lipinski rule of five, any molecule with a molecular weight less than 500 g/mol (MW $\leq$ 500 g/mol) is a feasible drug candidate (Chen et al., 2020). The molecular weights of the three potential compounds were 410.686, 394.687, and 412.702 g/moL for 28-demethyl-beta-amyrone, 24-Noroleana-3,12-diene, and stigmasterol, respectively. To be a plausible drug candidate, a compound's H-bond acceptors and H-bond donors should not be more than ten and five, respectively, according to the Lipinski rule of five (Alodeani et al., 2015). The numbers of H-bond acceptors were 1, 0, and 1, and the H-bond donors were 0, 0, and 1 for 28-demethyl-beta-amyrone, 24-Noroleana-3,12-diene, and stigmasterol, respectively. The topological polar surface area (TPSA) score must be within the range of 0 $Å^2$ to 140 $Å^2$ for being a potential drug candidate(Jagannathan, 2019). The TPSA scores were 17.07, 0.00, and 20.23 $Å^2$, whereas BBB permeability was 0.705, 0.848, and 0.771 for 28-demethyl-beta-amyrone, 24-noroleana-3,12-diene, and stigmasterol, respectively. The Human Intestinal Absorption were 96.643%, 96.674%, and 94.97%, respectively, for 28-demethyl-beta-amyrone, 24-Noroleana-3,12-diene, and stigmasterol confirming the high absorption rate of the selected three compounds in the intestine. Moreover, the three compounds were recognized as P-gp non-substrate in addition to appearing as non-toxic in conformity with AMES toxicity and hepatotoxicity

Table 1 The docking interactions of spike receptor-binding domain and top ligand molecules in molecular docking. The interactions were retrieved from the Discovery Studio software, where; A, PA, PS, H, indicates the alkyl, pi-alkyl, pi-sulfur, and hydrogen bond respectively.

Complex	Amino Acid Residues	Bond Type	Distance (Å)	Docking Energy (Kcal/mol) AutoDock Vina	Docking Energy (Kcal/mol) Dockthor	Docking Energy (Kcal/mol) SwissDock
	Phe342	H	2.02		−5.985	−7.38
	Leu368	H	2.46			
	Phe342	PA	5.20			
	Ser371	H	2.47			
	Trp436	H	2.07			
	Arg509	H	2.01			
	Trp508	H	2.44			
	Trp436	APS	3.99			
28-demethyl-beta-amyrone	Phe374	PA	4.82	−8.3		
	Trp436	PA	4.51			
	Phe338	H	2.01			
	Tyr365	H	2.46			
	Ser375	H	2.55			
	Asn437	H	2.20			
	Ile368	PA	5.20			
	Val511	PA	3.93			
	Ile434	PA	5.17			
	Phe342	H	2.18			
	Val367	H	2.54			
	Phe338	H	2.03			
	Leu368	H	2.46			
	Ser371	H	2.80			
24-Noroleana-3,12-diene	Phe342	PA	5.20		−6.002	−7.48
	Phe374	PA	5.17	−7.5		
	Asp364	H	2.54			
	Tyr365	H	2.46			
	Ile434	PA	5.37			
	Val511	PA	3.93			
	Leu335	H	2.61			
	Phe338	H	2.03		−5.712	−7.25
	Val341	H	2.14			
	Phe342	H	2.02			
	Leu368	H	2.46			
	Ser371	H	2.47			
	Leu368	A	4.87			
	Phe338	PA	4.69			
	Phe342	PA	4.96	−8.1		
	Phe374	PA	5.28			
	Asn334	H	2.63			
	Cys335	H	2.03			
	Tyr365	H	2.46			
	Val362	H	2.51			
	Cys336	PA	4.69			
	Ile358	PA	4.91			
	Ala363	PA	5.02			
	Ile434	PA	5.37			
	Val511	PA	3.93			

profiling. In addition, three potential molecules were thought to fulfill the Lipinski rule of five, with one violation in each compound; however, one violation is always acceptable for being a viable therapeutic candidate (Daina et al., 2017).

3.6. Molecular dynamics simulation

The molecular dynamics simulation of the docked complexes was conducted to analyze the structural stability and the equilibration of the ensemble across the atomistic simulations. Fig. 8 **(a)** demonstrates the root mean square deviations of the C-alpha atoms from the docked complexes. Fig. 8 **(a)** indicates that at the start of simulations, all three complexes, 28-demethyl-beta-amyrone, 24-Noroleana-3,12-diene, and stigmasterol exhibited an initially higher trend. This trend might have occurred as a result of the complexes' increased flexibility. The complexes attained a steady state after 10 ns of the simulation times. The stigmasterol had a somewhat

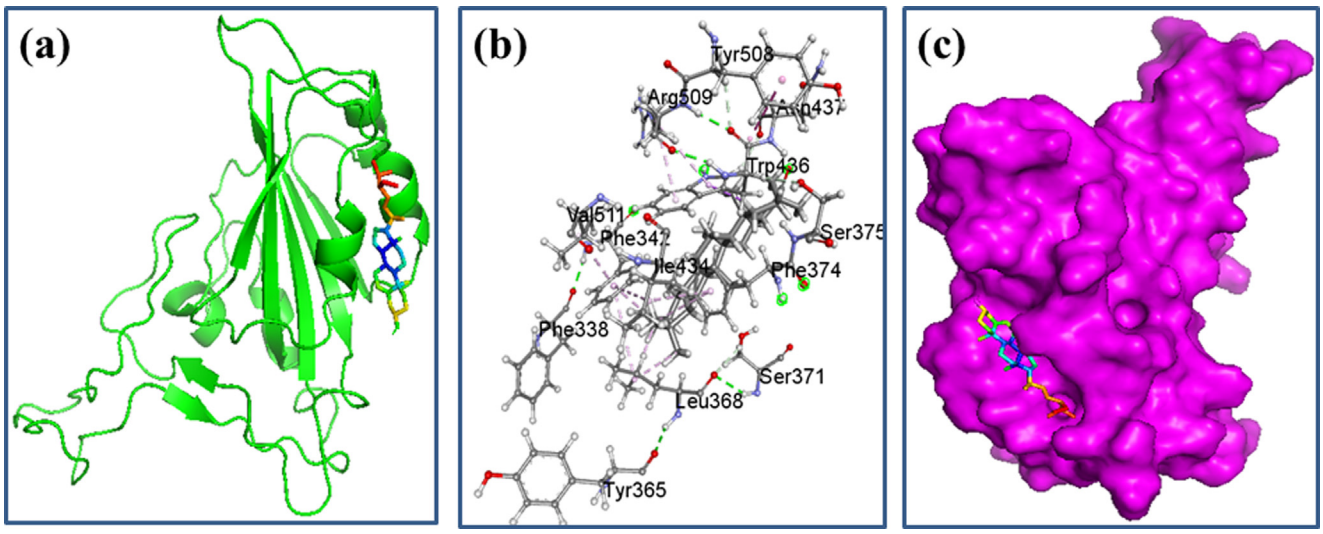

Fig. 5 Docking simulation between spike receptor-binding domain of SARs-CoV-2 and 28-demethyl-beta-amyrone, respectively, where (a) Cartoon view, (b) 3D view, and (c) Surface view.

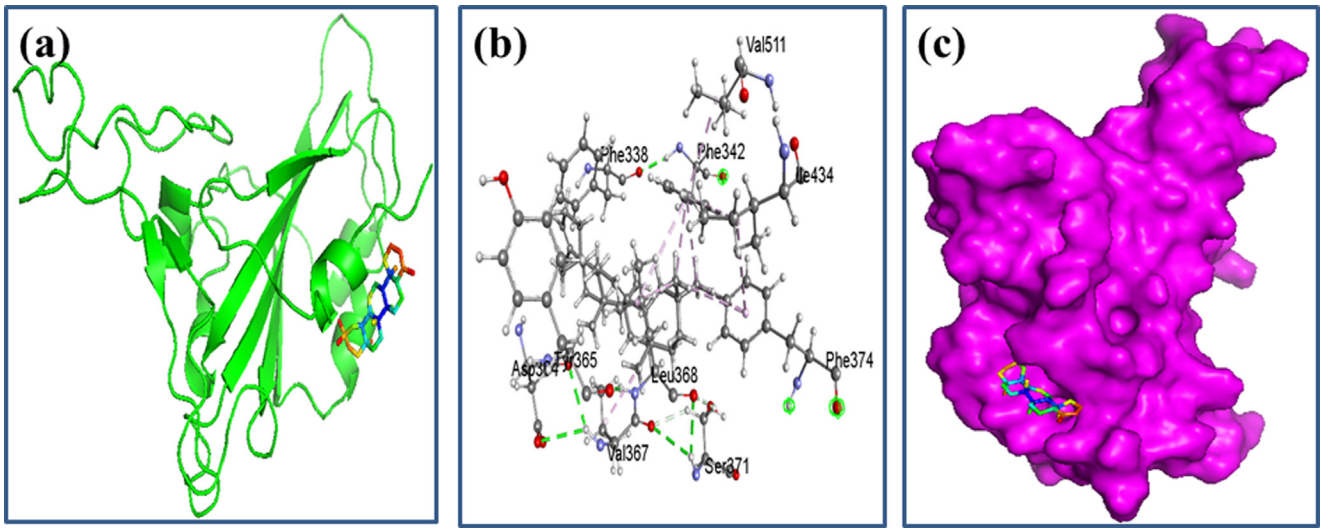

Fig. 6 Docking simulation between spike receptor-binding domain of SARS-CoV-2 and 24-Noroleana-3,12-diene respectively, where (a) Cartoon view, (b) 3D view, and (c) Surface view.

greater RMSD than the other two complexes at 40–60 ns, which could explain the higher flexibility of the complexes. The RMSD of all three complexes was less than 2.5, indicating that they have a stable and rigid overall profile. Furthermore, the stable and steady nature of the protein systems is defined by the hydrogen bond patterning of the simulating systems. The hydrogen bond for all three complexes, 28-demethyl-beta-amyrone, 24-Noroleana-3,12-diene, and stigmasterol, was stable and did not fluctuate much [Fig. 8 **(b)**].

Moreover, the solvent accessible surface area of the complexes was investigated to better understand the changes in the protein's surface area. The higher SASA, the more the surface area expands, and the lower the SASA, the more the protein is truncated. The 24-Noroleana-3,12-diene had a somewhat greater SASA at 40–45 ns times denoting the extension of the surface area of the complexes [Fig. 9 **(a)**]. However, the SASA of stigmasterol was lower than that of all three complexes, indicating that the complexes were more condensed with time. The radius of gyration of the complexes determines their liability and mobile nature. Higher Rg indicates that the complexes are more flexible. The 24-Noroleana-3, 12-diene had lower Rg than the other two complexes, which indicate a comparatively stable profile of these complexes [Fig. 9 **(b)**]. The other two complexes had minor variances, but they did not differ much.

4. Discussion

Currently, battling COVID-19 has become a major issue for the entire world due to the virus's global exposure. Moreover, the virus's breakout is becoming more severe and causing an

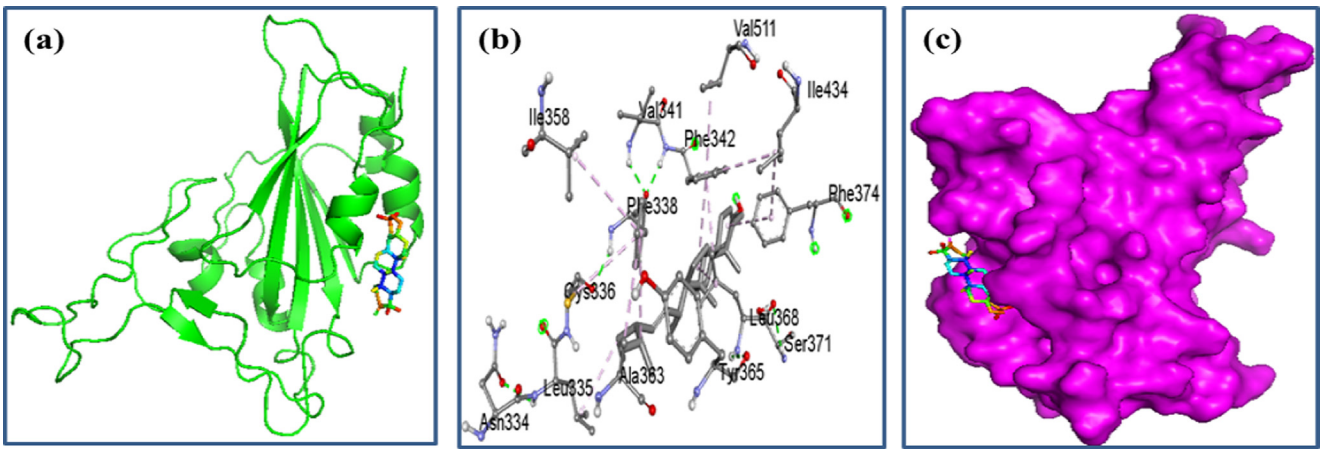

Fig. 7 Docking simulation between spike receptor-binding domain of SARS-CoV-2 and stigmasterol, respectively, where (a) Cartoon view, (b) 3D view, and (c) Surface view.

Table 2 Pharmacological assessment of the screened hit ligand molecules.

Parameters	28-demethyl-beta-amyrone	24-Noroleana-3,12-diene	Stigmasterol
Molecular Weight	410.686 g/mol	394.687 g/mol	412.702 g/mol
Num. H-bond acceptors	1	0	1
Num. H-bond donors	0	0	1
TPSA (S)	17.07 $Å^2$	0.00 $Å^2$	20.23 $Å^2$
BBB permeability	0.705	0.848	0.771
Human Intestinal Absorption	96.643 %	96.674 %	94.97 %
P-glycoprotein substrate	No	No	No
AMES Toxicity	No	No	No
Lipinski rule of five	Yes; 1 violation	Yes; 1 violation	Yes; 1 violation
Hepatotoxicity	No	No	No

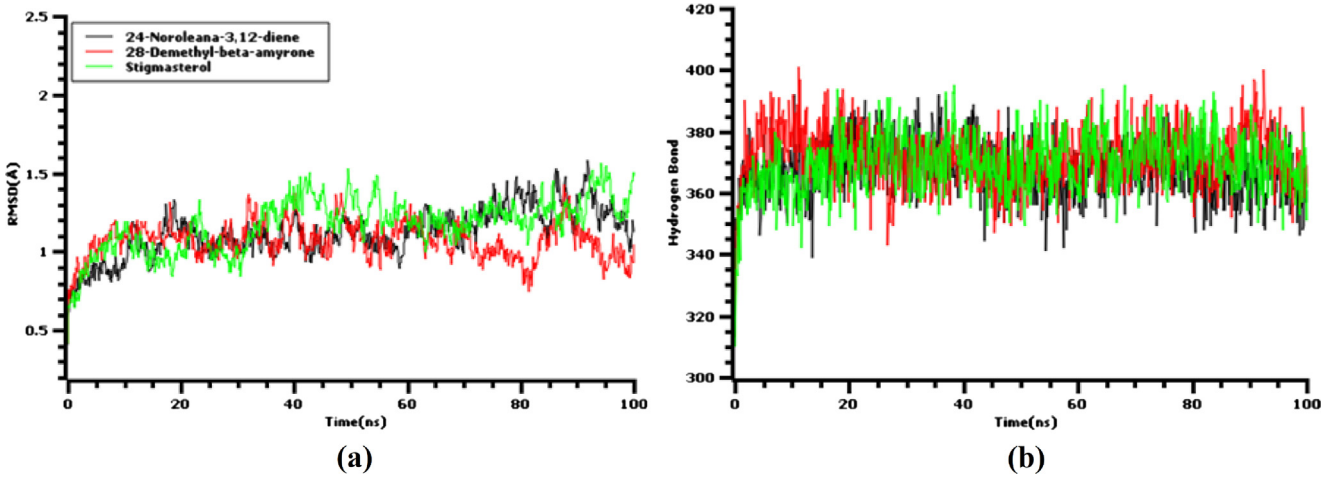

Fig. 8 The molecular dynamics simulation. (a) Root mean square deviation of the three docked complexes, (b) hydrogen bond of the docked complexes.

increasing number of deaths. Although many vaccines have been recognized by the WHO, vaccine adoption rates vary by country (Sallam, 2021), and vaccines are not readily available in poor countries, particularly in low-income countries. As of July 20, 2021, only 26.3% of the global population has received at least one dose of vaccine. In contrast, only 1.1% of people in poor countries are now under a vaccination program to administer at least one dose (https://ourworldindata.org /covidvaccinations?country = OWID WRL&fbclid = I

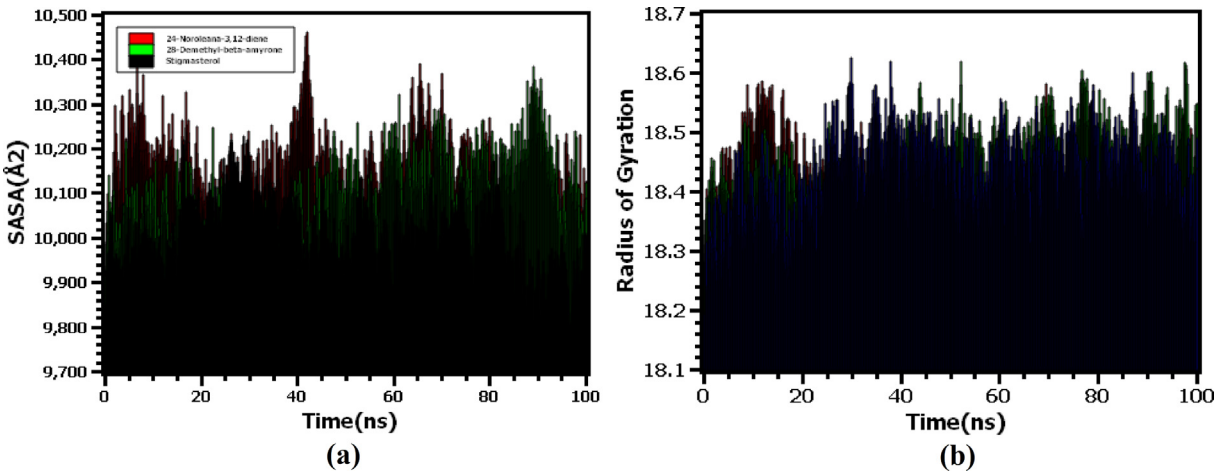

Fig. 9 The molecular dynamics simulations of (a) solvent accessible surface area, (b) radius of gyration of the complexes.

wAR0UFG9nExAHpRtFRBRV7wjprvuDz68REj LEhwBK9pVhOnDSQGrMtPXAR_Ew.

SARS-CoV-2 variants have been identified globally, and the U.S. Centers for Disease Control and Prevention (CDC) classifies them as variants of concern, variants of interest, and variants of significant consequence (Abdool Karim and de Oliveira, 2021). Variants are mostly created through virus mutations, and SARS-CoV-2 variants have recently been discovered in large numbers. Three of them, the B.1.1.7 variant, the 501Y.V2 variant, and the P.1 variant, have become important concerns since they have roughly 23, 23, and 35 mutations, respectively, and have spread rapidly throughout numerous nations. Those mutations are mostly found in the spike protein's receptor-binding domain, which improves the RBD's affinity for ACE-2. Several varieties can cause more serious infections, with some being able to spread faster than others and, more crucially, evade the host body's immune response, which grows after infection and despite immunization (Abdool Karim and de Oliveira, 2021; Walensky et al., 2021).

As a result, producing a traditional medicine by screening a new phytochemical component could be beneficial in treating the virus in this case. We therefore selected two mangrove plants' leaves and fruits and isolated their components to identify new lead molecules against SARS-CoV-2 using molecular docking and dynamics. Some studies have previously shown that natural plant chemicals can successfully combat pathogenic disease (Joshi et al., 2020; Khaerunnisa et al., 2020), and mangrove plants have also been used for therapeutic purposes since ancient times (Dahibhate et al., 2018).

The higher antioxidant activity of plants is a crucial factor in the creation of new drugs. The 2,2-diphenyl-1-picrylhydrazyl (DPPH) free radical scavenging assay is a good way to assess plant antioxidant activity (Choi et al., 2000). Furthermore, certain phytochemical substances have anticancer properties (XiaoPing et al., 2009). In the current investigation, both *Pistacia integerrima* and *Pandanus odorifer* leaf extracts had higher antioxidant activity (142.10 g/mL and 112.50 g/mL, respectively) than their fruit extracts (173.58 g/mL and 292.71 g/mL, respectively) (see Fig. 1). In vitro brine shrimp fatality experiments are also useful for determining the toxicity of plants (Carballo et al., 2002). Both *Pistacia integerrima* and *Pandanus odorifer* leaf extracts showed less toxicity in toxicity tests (95.54 g/mL and 117.00 g/mL, respectively) than their fruits extracts (82.27 g/mL and 67.51 g/mL, respectively) (Figure-2). The GC–MS analysis of *Pistacia integerrima* and *Pandanus odorifer* plant showed 145 phytochemical compounds. Because the antioxidant content of both plant leaves was higher and the toxicity of their fruits extract was lower, these leaves can be considered biological agents with a lot of potential for molecular docking investigations. Finally, potent phytochemicals against the spike receptor-binding domain protein of SARS CoV-2 were identified through computational research.

Plant antioxidants can protect cells from damage by free radicals, and molecular docking studies are used to determine the interaction dynamics of a protein complex (Mahmud et al., 2021b). The results of these two investigations were combined to determine the pharmacological characteristics of the leaf extracts. Antioxidant activity can be checked via molecular docking under *in silico* conditions, but in this study, the antioxidant activity was assessed under lab conditions and molecular docking was used only to assess the properties of phytochemicals derived from *Pistacia integerrima* and *Pandanus odorifer* plants against target proteins.

A structure-based computer-aided virtual screening technique known as molecular docking effectuates a distinct amalgamation of positions, orientations, and conformations through the assessment of the interaction between a protein and a plausible drug molecule utilizing computer-inured three-dimensional structures with the purpose of structure-premised drug design (Chaudhary and Mishra, 2016; Roblin, 1953). In the computational drug discovery process, protein pliability is important for ligand binding. If biologists or researchers seek to figure out how a protein, ligand, or other molecule works, the motions of those unique biomolecules will be quite helpful and provide a wealth of information about their functions. The grandiose diversity of essential bio molecular systems, such as conformational variation, protein flexion, ligand nexus, and eliciting atomic sites, can be captured using a simulation (Hollingsworth and Dror, 2018).

In docking studies, binding at the active regions of proteins causes the targeted protein to be inhibited (Mahmud et al., 2021c, 2021b). The complexes 24-Noroleana-3,12-diene and

stigmasterol had non-bonded contacts with the active points Phe374 in this investigation, as well as many interactions around the active points of the targeted protein, which could be responsible for the target protein's inhibition. In addition, numerous descriptors derived from simulated trajectories for docked structures suggested tight conformations and a less flexible character of the complexes. The binding stability of the complexes is correlated with the root mean square deviations for the C-alpha atoms of the docked complexes, radius of gyrations, solvent accessible surface area, root mean square fluctuations and hydrogen bond of the systems. In addition, the top three potential candidates fulfilled the Lipinski rule of five with one violation in each compound, where each compound has a molecular weight less than 500 g/mol, and the H-bond acceptors and H-bond donors are not more than ten and five, respectively. Though each molecule has only one violation of the Lipinski rule of five, which is MlogP > 4.15, one violation is nevertheless always acceptable for being a feasible therapeutic candidate (Daina et al., 2017). As a result, chemicals from *Pistacia integerrima* and *Pandanus odorifer* plants may inhibit the receptor domain of the spike protein. These findings must be confirmed through wet-lab synthesis and additional in vivo investigations.

5. Conclusion

Plants, as opposed to synthetic substances, are becoming a more viable source for therapeutic application due to their comprehensive appearance, reduced side effects, and broad specificity. Due to the scarcity of effective vaccinations, the mortality rate from the COVID-19 pandemic is rising by the day. Consequently, we tested the efficiency of leaf and fruit extracts from two mangrove plants (*Pistacia integerrima* and *Pandanus odorifer*) as potential SARS-CoV-2 inhibitors. Both plants had significant antioxidant and cytotoxicity effects when methanolic extracts of leaves and fruits were tested. The molecular docking study identified three potential compounds, 28-demethyl-beta-amyrone, 24-Noroleana-3,12-diene, and stigmasterol, as having the maximum binding energy in complexes with the spike receptor-binding domain protein of SARS-CoV-2. This study may aid researchers in developing a viable therapy for SARS-CoV-2. As a result, additional in vivo and in vitro validation is required for the confirmation and safety profiles of the findings of this study.

Funding

This research was partially supported by the Ministry of Science and Technology, Government of the People's Republic of Bangladesh. The authors are also grateful to the Deanship of Scientific Research at King Khalid University for funding this study through the Small Research Group Project, under grant number GRP/340 /42.

CRediT authorship contribution statement

Gobindo Kumar Paul: Conceptualization, Data curation, Formal analysis, Investigation, Methodology, Writing – original draft, Writing – review & editing. **Shafi Mahmud:** Conceptualization, Data curation, Formal analysis, Investigation, Methodology, Writing – original draft, Writing – review & editing. **Afaf A Aldahish:** Funding acquisition, Project administration. **Mirola Afroze:** Formal analysis, Investigation. **Swagota Briti Ray Gupta:** Data curation, Methodology. **Mahmudul Hasan Razu:** Formal analysis, Investigation. **Shahriar Zaman:** Resources, Writing – review & editing. **Md. Salah Uddin:** Resources, Writing – review & editing. **Mohammed H Nahari:** Data curation, Methodology. **Mohammed Merae Alshahrani:** Data curation, Methodology. **Mohammed Abdul Rahman Alshahrani:** Data curation, Methodology. **Mala Khan:** Project administration, Resources, Supervision, Writing – review & editing. **Md. Abu Saleh:** Conceptualization, Funding acquisition, Project administration, Resources, Software, Supervision, Writing – review & editing.

Declaration of Competing Interest

The authors declare that they have no known competing financial interests or personal relationships that could have appeared to influence the work reported in this paper.

Appendix A. Supplementary material

Supplementary data to this article can be found online at https://doi.org/10.1016/j.arabjc.2021.103600.

References

A. Hussein, R., A. El-Anssary, A., 2019. Plants Secondary Metabolites: The Key Drivers of the Pharmacological Actions of Medicinal Plants. Herb. Med. 10.5772/intechopen.76139.

A., S., M., D., D., B., A., C., C., B., G., G., E., B., D., T., 2017. In vitro evaluation of the antioxidant, cytoprotective, and antimicrobial properties of essential oil from Pistacia vera L. Variety Bronte Hull. Int. J. Mol. Sci. 18.

Abdool Karim, S.S., de Oliveira, T., 2021. New SARS-CoV-2 Variants — Clinical, Public Health, and Vaccine Implications. N. Engl. J. Med. 384, 1866–1868. https://doi.org/10.1056/nejmc2100362.

Achakzai, J.K., Anwar Panezai, M., Kakar, M.A., Kakar, A.M., Kakar, S., Khan, J., Khan, N.Y., Khilji, I., Tareen, A.K., 2019. In Vitro Anticancer MCF-7, Anti-Inflammatory, and Brine Shrimp Lethality Assay (BSLA) and GC-MS Analysis of Whole Plant Butanol Fraction of Rheum ribes (WBFRR). Biomed Res. Int. 2019. https://doi.org/10.1155/2019/3264846.

Afrose, S., Hasan, R., Sharmin, M., Shimu, S., 2021. Antiviral peptides against the main protease of SARS-CoV- 2: A molecular docking and dynamics study. Arab. J. Chem. 103315. https://doi.org/10.1016/j.arabjc.2021.103315.

Alodeani, E.A., Arshad, M., Izhari, M.A., 2015. Anti-uropathogenic activity, drug likeness, physicochemical and molecular docking assessment of (E-)-N0-(substituted-benzylidene)-2-(quinolin-8-yloxy) acetohydrazide. Asian Pac. J. Trop. Biomed. 5, 676–683. https://doi.org/10.1016/j.apjtb.2015.04.010.

C., P., M.E., M., A.T., P., G., D.C., V., P., 2020. The "Three Italy" of the COVID-19 epidemic and the possible involvement of SARS-CoV-2 in triggering complications other than pneumonia. J. Neurovirol.

Carballo, J.L., Hernández-Inda, Z.L., Pérez, P., García-Grávalos, M. D., 2002. A comparison between two brine shrimp assays to detect in vitro cytotoxicity in marine natural products. BMC Biotechnol. 2. https://doi.org/10.1186/1472-6570-2-17.

Chaudhary, K.K., Mishra, N., 2016. A Review on Molecular Docking: Novel Tool for Drug Discovery. JSM Chem 4, 1029.

Chen, X., Li, H., Tian, L., Li, Q., Luo, J., Zhang, Y., 2020. Analysis of the Physicochemical Properties of Acaricides Based on Lipinski's Rule of Five. J. Comput. Biol. 27, 1397–1406. https://doi.org/10.1089/cmb.2019.0323.

Choi, H.S., Sun Song, H., Ukeda, H., Sawamura, M., 2000. Radical-scavenging activities of citrus essential oils and their components: Detection using 1,1-diphenyl-2-picrylhydrazyl. J. Agric. Food Chem. https://doi.org/10.1021/jf000227d.

Chowdhury, K.H., Chowdhury, M.R., Mahmud, S., Tareq, A.M., Hanif, N.B., Banu, N., Ali Reza, A.S.M., Emran, T. Bin, Simal-Gandara, J., 2021. Drug repurposing approach against novel coronavirus disease (COVID-19) through virtual screening targeting SARS-CoV-2 main protease. Biology (Basel). 10, 1–14. https://doi.org/10.3390/biology10010002.

Corrêa Giron, C., Laaksonen, A., Barroso da Silva, F.L., 2020. On the interactions of the receptor-binding domain of SARS-CoV-1 and SARS-CoV-2 spike proteins with monoclonal antibodies and the receptor ACE2. Virus Res. 285,. https://doi.org/10.1016/j.virusres.2020.198021 198021.

Dahibhate, N.L., Saddhe, A.A., Kumar, K., 2018. Mangrove Plants as a Source of Bioactive Compounds: A Review. Nat. Prod. J. 9, 86–97. https://doi.org/10.2174/2210315508666180910125328.

Daina, A., Michielin, O., Zoete, V., 2017. SwissADME: a free web tool to evaluate pharmacokinetics, drug-likeness and medicinal chemistry friendliness of small molecules. Sci. Rep. 7, 42717.

DeLano, W.L., 2002. Pymol: An open-source molecular graphics tool. CCP4 Newsl. protein Crystallogr. 40, 82–92.

Ebrahim, S.H., Ahmed, Q.A., Gozzer, E., Schlagenhauf, P., Memish, Z.A., 2020. COVID-19 and community mitigation strategies in a pandemic. BMJ 368. https://doi.org/10.1136/bmj.m1066.

Essmann, U., Perera, L., Berkowitz, M.L., Darden, T., Lee, H., Pedersen, L.G., 1995. A smooth particle mesh Ewald method. J. Chem. Phys. 103, 8577–8593. https://doi.org/10.1063/1.470117.

Gao, Y.D., Huang, J.F., 2011. An extension strategy of Discovery Studio 2.0 for non-bonded interaction energy automatic calculation at the residue level]. Dongwuxue. Yanjiu. 32, 262–266. https://doi.org/10.3724/SP.J.1141.2011.03262.

Grosdidier, A., Zoete, V., Michielin, O., 2011. SwissDock, a protein-small molecule docking web service based on EADock DSS. Nucleic Acids Res. https://doi.org/10.1093/nar/gkr366.

Hanwell, M.D., Curtis, D.E., Lonie, D.C., Vandermeerschd, T., Zurek, E., Hutchison, G.R., 2012. Avogadro: An advanced semantic chemical editor, visualization, and analysis platform. J. Cheminform. 4. https://doi.org/10.1186/1758-2946-4-17.

Harrach, M.F., Drossel, B., 2014. Structure and dynamics of TIP3P, TIP4P, and TIP5P water near smooth and atomistic walls of different hydroaffinity. J. Chem. Phys. 140, 174501.

He, Y., Zhou, Y., Liu, S., Kou, Z., Li, W., Farzan, M., Jiang, S., 2004. Receptor-binding domain of SARS-CoV spike protein induces highly potent neutralizing antibodies: Implication for developing subunit vaccine. Biochem. Biophys. Res. Commun. 324, 773–781. https://doi.org/10.1016/j.bbrc.2004.09.106.

Hollingsworth, S.A., Dror, R.O., 2018. Molecular Dynamics Simulation for All. Neuron 99, 1129–1143. https://doi.org/10.1016/j.neuron.2018.08.011.

Ilahi, I., Samar, S., Khan, I., Ahmad, I., 2013. In vitro antioxidant activities of four medicinal plants on the basis of DPPH free radical scavenging. Pak. J. Pharm. Sci. 26, 949–952.

Jagannathan, R., 2019. Characterization of Drug-like Chemical Space for Cytotoxic Marine Metabolites Using Multivariate Methods. ACS Omega 4, 5402–5411. https://doi.org/10.1021/acsomega.8b01764.

Jaghoori, M.M., Bleijlevens, B., Olabarriaga, S.D., 2016. 1001 Ways to run AutoDock Vina for virtual screening. J. Comput. Aided. Mol. Des. 30, 237–249. https://doi.org/10.1007/s10822-016-9900-9.

Joshi, T., Joshi, T., Sharma, P., Mathpal, S., Pundir, H., 2020. In silico screening of natural compounds against COVID-19 by targeting Mpro and ACE2 using molecular docking 4529–4536.

Khaerunnisa, S., Kurniawan, H., Awaluddin, R., Suhartati, S., 2020. Potential Inhibitor of COVID-19 Main Protease (M pro) from Several Medicinal Plant Compounds by Molecular Docking Study. Preprints, 1–14.

Kim, C., Ryu, D.K., Lee, J., Kim, Y. Il, Seo, J.M., Kim, Y.G., Jeong, J.H., Kim, M., Kim, J.I., Kim, P., Bae, J.S., Shim, E.Y., Lee, M.S., Kim, M.S., Noh, H., Park, G.S., Park, J.S., Son, D., An, Y., Lee, J. N., Kwon, K.S., Lee, J.Y., Lee, H., Yang, J.S., Kim, K.C., Kim, S. S., Woo, H.M., Kim, J.W., Park, M.S., Yu, K.M., Kim, S.M., Kim, E.H., Park, S.J., Jeong, S.T., Yu, C.H., Song, Y., Gu, S.H., Oh, H., Koo, B.S., Hong, J.J., Ryu, C.M., Park, W.B., Oh, M. don, Choi, Y.K., Lee, S.Y., 2021. A therapeutic neutralizing antibody targeting receptor binding domain of SARS-CoV-2 spike protein. Nat. Commun. 12, 1–10. 10.1038/s41467-020-20602-5.

Kim, S., Thiessen, P.A., Bolton, E.E., Chen, J., Fu, G., Gindulyte, A., Han, L., He, J., He, S., Shoemaker, B.A., Wang, J., Yu, B., Zhang, J., Bryant, S.H., 2016. PubChem substance and compound databases. Nucleic Acids Res. 44, D1202–D1213. https://doi.org/10.1093/nar/gkv951.

Krieger, E., Vriend, G., 2015. New ways to boost molecular dynamics simulations. J. Comput. Chem. 36, 996–1007. https://doi.org/10.1002/jcc.23899.

Lan, J., Ge, J., Yu, J., Shan, S., Zhou, H., Fan, S., Zhang, Q., Shi, X., Wang, Q., Zhang, L., Wang, X., 2020. Structure of the SARS-CoV-2 spike receptor-binding domain bound to the ACE2 receptor. Nature 581, 215–220. https://doi.org/10.1038/s41586-020-2180-5.

Land, H., Humble, M.S., 2018. YASARA: A tool to obtain structural guidance in biocatalytic investigations. Methods Mol. Biol. 1685, 43–67. https://doi.org/10.1007/978-1-4939-7366-8_4.

Li, F., Li, W., Farzan, M., Harrison, S.C., 2005. Structure of SARS coronavirus spike receptor-binding domain complexed with receptor. Science (80-.). 309, 1864–1868.

Liu, X., Zhao, M., Wang, J., Yang, B., Jiang, Y., 2008. ARTICLE IN PRESS Antioxidant activity of methanolic extract of emblica fruit (Phyllanthus emblica L .) from six regions in China 21, 219–228. 10.1016/j.jfca.2007.10.001

Machhi, J., Herskovitz, J., Senan, A.M., Dutta, D., Nath, B., Oleynikov, M.D., Blomberg, W.R., Meigs, D.D., Hasan, M., Patel, M., Kline, P., Chang, R.C., Chang, L., Gendelman, H.E., Kevadiya, B.D., 2020. The Natural History , Pathobiology , and Clinical Manifestations of SARS-CoV-2 Infections 359–386.

Mahmud, S., Biswas, S., Paul, G.K., Mita, M.A., Promi, M.M., Afrose, S., Hasan, M.R., Zaman, S., Uddin, M.S., Dhama, K., Emran, T. Bin, Saleh, M.A., Simal-Gandara, J., 2021a. Plant-based phytochemical screening by targeting main protease of sars-cov-2 to design effective potent inhibitors. Biology (Basel). 10. https://doi.org/10.3390/biology10070589.

Mahmud, S., Hasan, M.R., Biswas, S., Paul, G.K., Afrose, S., Mita, M.A., Sultana Shimu, M.S., Promi, M.M., Hani, U., Rahamathulla, M., Khan, M.A., Zaman, S., Uddin, M.S., Rahmatullah, M., Jahan, R., Alqahtani, A.M., Saleh, M.A., EmranBin, T., 2021g. Screening of Potent Phytochemical Inhibitors Against SARS-CoV-2 Main Protease. An Integrative Computational Approach. Front. Bioinforma. 1 https://doi.org/10.3389/fbinf.2021.717141.

Mahmud, S., Mita, M.A., Biswas, S., Paul, G.K., Promi, M.M., Afrose, S., Hasan, R., Shimu, S.S., Zaman, S., Uddin, S., Tallei, T. E., EmranBin, T., Saleh, A., 2021f. Molecular docking and dynamics study to explore phytochemical ligand molecules against the main protease of SARS-CoV-2 from extensive phytochemical datasets. Expert Rev. Clin. Pharmacol. 14, 1305–1315 https://doi.org/10.1080/17512433.2021.1959318.

Mahmud, S., Paul, G.K., Afroze, M., Islam, S., Gupt, S.B.R., Razu, M.H., Biswas, S., Zaman, S., Uddin, M.S., Khan, M., Cacciola, N. A., Emran, T. Bin, Saleh, M.A., Capasso, R., Simal-Gandara, J., 2021b. Efficacy of phytochemicals derived from avicennia officinalis for the management of covid-19: A combined in silico and biochemical study. Molecules 26. https://doi.org/10.3390/molecules26082210.

Mahmud, S., Paul, G.K., Biswas, S., Afrose, S., Mita, M.A., Hasan, M.R., Shimu, M.S.S., Hossain, A., Promi, M.M., Ema, F.K., Chidambaram, K., Chandrasekaran, B., Alqahtani, A.M., Emran, T. Bin, Saleh, M.A., 2021c. Prospective Role of Peptide-Based Antiviral Therapy Against the Main Protease of SARS-CoV-2. Front. Mol. Biosci. 8. https://doi.org/10.3389/fmolb.2021.628585.

Mahmud, S., Rafi, O., Paul, G.K., Promi, M.M., Sharmin, M., Shimu, S., Biswas, S., Emran, T. Bin, Dhama, K., 2021d. Designing a multi - epitope vaccine candidate to combat MERS - CoV by employing an immunoinformatics approach. Sci. Rep. 1–21. https://doi.org/10.1038/s41598-021-92176-1.

Mahmud, S., Uddin, M.A.R., Paul, G.K., Shimu, M.S.S., Islam, S., Rahman, E., Islam, A., Islam, M.S., Promi, M.M., Emran, T. Bin, Saleh, M.A., 2021e. Virtual screening and molecular dynamics simulation study of plant-derived compounds to identify potential inhibitors of main protease from SARS-CoV-2. Brief. Bioinform. 22, 1402–1414. https://doi.org/10.1093/bib/bbaa428.

Nguyen, N.T., Nguyen, T.H., Pham, T.N.H., Huy, N.T., Bay, M. Van, Pham, M.Q., Nam, P.C., Vu, V.V., Ngo, S.T., 2020. Autodock Vina Adopts More Accurate Binding Poses but Autodock4 Forms Better Binding Affinity. J. Chem. Inf. Model. 60, 204–211. https://doi.org/10.1021/acs.jcim.9b00778.

Pant, S., Samant, S.S., 2010. Ethnobotanical Observations in the Mornaula Reserve Forest of Kumoun, West Himalaya. India. Ethnobot. Leafl., 193–217

Pires, D.E.V., Blundell, T.L., Ascher, D.B., 2015. pkCSM: Predicting small-molecule pharmacokinetic and toxicity properties using graph-based signatures. J. Med. Chem. 58, 4066–4072. https://doi.org/10.1021/acs.jmedchem.5b00104.

Pramanik, S.K., Mahmud, S., Paul, G.K., Jabin, T., Naher, K., Uddin, M.S., Zaman, S., Saleh, M.A., 2021. Fermentation optimization of cellulase production from sugarcane bagasse by Bacillus pseudomycoides and molecular modeling study of cellulase. Curr. Res. Microb. Sci. 2,. https://doi.org/10.1016/j.crmicr.2020.100013 100013.

Profiles, C., Attributes, B., Obaidullah, A.J., Alanazi, M.M., Alsaif, N. A., Mahdi, W.A., Fantoukh, O.I., Tareq, A.M., Sami, S.A., Alqahtani, A.M., Emran, T. Bin, 2021. Deeper Insights on Cnesmone javanica Blume Leaves Extract : Pharmacology and Molecular Docking.

Rakib, A., Nain, Z., Sami, S.A., Mahmud, S., Islam, A., Ahmed, S., Siddiqui, A.B.F., Babu, S.M.O.F., Hossain, P., Shahriar, A., Nainu, F., Emran, T. Bin, Simal-Gandara, J., 2021. A molecular modelling approach for identifying antiviral selenium-containing heterocyclic compounds that inhibit the main protease of SARS-CoV-2: An in silico investigation. Brief. Bioinform. 22, 1476–1498. https://doi.org/10.1093/bib/bbab045.

Roblin, R.O., 1953. Medicinal chemistry. Chem. Eng. News 31, 48–49. https://doi.org/10.1021/cen-v031n001.p048.

Sallam, M., 2021. COVID-19 vaccine hesitancy worldwide: A concise systematic review of vaccine acceptance rates. Vaccines 9, 1–15. https://doi.org/10.3390/vaccines9020160.

Santos, K.B., Guedes, I.A., Karl, A.L.M., Dardenne, L.E., 2020. Highly Flexible Ligand Docking: Benchmarking of the DockThor Program on the LEADS-PEP Protein-Peptide Data Set. J. Chem. Inf. Model. https://doi.org/10.1021/acs.jcim.9b00905.

Satarker, S., Nampoothiri, M., 2020. Structural Proteins in Severe Acute Respiratory Syndrome Coronavirus-2. Arch. Med. Res. 51, 482–491. https://doi.org/10.1016/j.arcmed.2020.05.012.

Shang, J., Ye, G., Shi, K., Wan, Y., Luo, C., Aihara, H., Geng, Q., Auerbach, A., Li, F., 2020. Structural basis of receptor recognition by SARS-CoV-2. Nature 581, 221–224. https://doi.org/10.1038/s41586-020-2179-y.

Sharma, O.P., Bhat, T.K., 2009. DPPH antioxidant assay revisited. Food Chem. 113, 1202–1205. https://doi.org/10.1016/j.foodchem.2008.08.008.

Trott, O., Olson, A.J., 2010. AutoDock Vina: improving the speed and accuracy of docking with a new scoring function, efficient optimization, and multithreading. J. Comput. Chem. 31, 455–461.

Uddin, Z., Paul, A., Rakib, A., Sami, S.A., Mahmud, S., Rana, S., Hossain, S., Tareq, A.M., Dutta, M., Emran, T. Bin, Simal-Gandara, J., 2021. Chemical profiles and pharmacological properties with in silico studies on elatostema papillosum wedd. Molecules 26. https://doi.org/10.3390/molecules26040809.

Walensky, R.P., Walke, H.T., Fauci, A.S., 2021. SARS-CoV-2 Variants of Concern in the United States-Challenges and Opportunities. JAMA - J. Am. Med. Assoc. 325, 1037–1038. https://doi.org/10.1001/jama.2021.2294.

Wang, J., Wolf, R.M., Caldwell, J.W., Kollman, P.A., Case, D.A., 2004. Development and testing of a general Amber force field. J. Comput. Chem. 25, 1157–1174. https://doi.org/10.1002/jcc.20035.

Wavare, S.H., Gade, R.M., Shitole, A. V., 2017. Antifungal efficacy of floral extracts, biocontrol agents and fungicides against Fusarium oxysporum f. sp. ciceri. Indian Phytopathol. 70, 191–199. 10.24838/ip.2017.v70.i2.70615.

XiaoPing, C., Yan, C., ShuiBing, L., YouGuo, C., JianYun, L., LanPing, L., 2009. Free radical scavenging of Ganoderma lucidum polysaccharides and its effect on antioxidant enzymes and immunity activities in cervical carcinoma rats. Carbohydr. Polym. https://doi.org/10.1016/j.carbpol.2009.01.009.

Yuan, M., Liu, H., Wu, N.C., Wilson, I.A., 2021. Recognition of the SARS-CoV-2 receptor binding domain by neutralizing antibodies. Biochem. Biophys. Res. Commun. 538, 192–203. https://doi.org/10.1016/j.bbrc.2020.10.012.